JOURNAL OF CATALYSIS 88, 81–88 (1984)

Deactivation of Copper, Nickel, and Cobalt Catalysts by Interaction with Aliphatic Amines

ALFONS BAIKER,[1] DANIELE MONTI, AND YUAN SONG FAN

Department of Industrial and Engineering Chemistry, Swiss Federal Institute of Technology (ETH), CH-8092 Zurich, Switzerland

Received February 23, 1983; revised August 8, 1983

The deactivation of alumina-supported and unsupported copper, nickel, and cobalt catalysts resulting from interaction with aliphatic amines was studied using the catalyzed disproportionation of methylamine and dimethylamine as test reactions. Temperature-programmed desorption (TPD) and surface reaction (TPSR) studies performed with the deactivated catalyst samples indicate that three different deactivation processes have to be considered, namely the formation of metal nitride, and the formation of metal carbide and carbonaceous deposits. With copper only nitride formation is observed. With nickel and cobalt all three deactivation processes can occur at temperatures used for catalytic disproportionation or amination. Hydrogen prevents metal nitride formation and inhibits the formation of metal carbide and carbonaceous deposits. TPSR studies carried out with a mixture of hydrogen in nitrogen showed for both the deactivated Ni/Al_2O_3 and Co/Al_2O_3 two maxima in the methane evolution curve, indicating the coexistence of carbon species with different reactivity towards hydrogen. The more reactive carbon species, probably consisting of chemisorbed carbon atoms and metal carbide, were unstable at high temperature (770 K), and slowly converted into a less reducible form.

INTRODUCTION

Catalytic amination of alcohols (*1–4*) and disproportionation of amines (*5, 6*) using supported metal catalysts is usually carried out in the presence of hydrogen. Without hydrogen a severe catalyst deactivation is often observed. It has recently been shown (*7*) that, in the absence of hydrogen, copper catalysts are deactivated by the formation of copper nitride. Copper nitride forms easily when copper interacts with the ammonia originating from the disproportionation of the reactant amine. Differential scanning calorimetry (DSC) and temperature-programmed desorption (TPD) measurements performed on nickel and cobalt catalysts, after exposure to ammonia, indicated that a surface metal nitride can also form on these catalysts. This led us to investigate in more depth the deactivation occurring on copper, nickel, and cobalt, which are three widely used amination catalysts. The metal-catalyzed disproportionation of methylamines is employed as a test reaction, and temperature-programmed desorption (TPD) and surface reaction (TPSR) are utilized to study the interaction of dimethylamine with the alumina-supported as well as the unsupported copper, nickel, and cobalt.

EXPERIMENTAL

Catalysts. The alumina-supported metal catalysts were prepared from aqueous solutions of the metal nitrates and aluminum hydroxide as described elsewhere (*8*) and the pure metal powders were prepared by conventional precipitation methods. The catalysts were reduced by heating at a rate of 5 K/min to the reduction temperature in a mixture of 6% hydrogen in nitrogen. After attaining the reduction temperature, a pure hydrogen flux was used to complete the reduction, generally overnight. The reduction temperatures employed were Cu/Al_2O_3 (470 K); Ni/Al_2O_3 (670 K); Co/Al_2O_3 (745 K); Cu (470 K); Ni (545 K); and Co (545 K). Some properties of the catalysts employed are listed in Table 1.

Deactivation studies. The catalyst deac-

---

[1] To whom all correspondence should be addressed.

0021-9517/84 $3.00

TABLE 1

Properties of Catalysts Used

Catalyst	Metal load (wt%)	Mean metal[a] particle size (nm)	BET-surface area (m^2/g)
Cu	—	31	8.8
Ni	—	32	11.3
Co	—	23	17.0
Cu/γ-alumina	43	15	69
Ni/γ-alumina	40	6.2	198
Co/γ-alumina	50	—	130
γ-Alumina	—	—	350

[a] Determined by X-ray diffraction line broadening after reduction.

tivation was investigated in a continuous fixed bed reactor. The general experimental details have been described previously (*7*). The experiments were started with a mixture of the reactant amine (monomethylamine or dimethylamine) in helium and hydrogen. After nearly stable conditions were attained the hydrogen was replaced by additional helium until the conversion of the amine again reached an almost constant value, indicating that the deactivation became very slow. Then, the additional helium was replaced again by hydrogen to study the reactivation.

TPD and TPSR measurements. The apparatus used for the TPD and TPSR measurements on the deactivated catalysts has been described in Refs. (*9*, *10*), respectively. The TPD and TPSR measurements were performed under the following conditions: sample weight 50 mg; heating rate 0.167 K/s; total pressure 96.5 kPa. The helium flow rate used in the TPD measurements was 1.67 ml (NTP)/s. TPSR was performed with a mixture of 6 mol% hydrogen in nitrogen at a flow rate of 1.25 ml (NTP)/s. Special care was taken to transfer the deactivated catalyst sample from the reactor to the TPD/TPSR-apparatus without exposure to air.

X-Ray diffraction. X-Ray diffraction patterns of the catalyst samples were obtained with a Norelco (Philips) X-ray diffractometer using Cu*Kα* radiation. Correction to the observed line breadth for instrumental broadening was made using the curves given by Rau (*11*).

RESULTS AND DISCUSSION

A. Deactivation Studies

In order to investigate the deactivation of the catalysts during disproportionation of the amines, experiments were performed in the flow reactor. Starting with either dimethylamine or monomethylamine, a mixture of trimethylamine, dimethylamine, monomethylamine, and ammonia was obtained through the reactions

$$2(CH_3)_2NH \rightleftharpoons CH_3NH_2 + (CH_3)_3N \quad (1)$$

$$2(CH_3)NH_2 \rightleftharpoons (CH_3)_2NH + NH_3 \quad (2)$$

$$(CH_3)_3N + NH_3 \rightleftharpoons (CH_3)_2NH + CH_3NH_2 \quad (3)$$

Only two of these reactions are linearly independent. Equilibrium compositions of methylamines and ammonia starting from monomethylamine and dimethylamine were reported previously (*4*).

In addition to disproportionation the formation of methane was observed with the nickel and cobalt catalysts.

$$(CH_3)_2NH + H_2 \rightleftharpoons CH_4 + CH_3NH_2 \quad (4)$$

$$CH_3NH_2 + H_2 \rightleftharpoons CH_4 + NH_3 \quad (5)$$

During disproportionation with the copper catalyst, no formation of methane or other hydrocracking products was observed, indicating that hydrocracking did not take place to a significant extent on this catalyst under the conditions given. The disproportionation and hydrocracking activity of the alumina-supported metal catalysts could completely be attributed to the supported metal; pure alumina support material, pretreated in the same way as the alumina-supported metal catalysts, did not show any

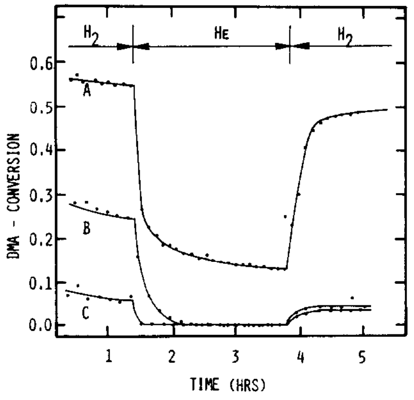

FIG. 1. Deactivation of alumina-supported metal catalysts during disproportionation of dimethylamine (DMA). (A) Cu/Al_2O_3; (B) Ni/Al_2O_3; (C) Co/Al_2O_3. Conditions: catalyst load, 1 g; temperature, 510 K; molar feed rates (mol s^{-1}): DMA, 1.65×10^{-5}; helium, 1.06×10^4; hydrogen or helium, 3.01×10^{-5}; total pressure, 100 kPa.

activity for the disproportionation or hydrocracking of the methylamines at 510 K.

Figures 1 and 2 show the deactivation behavior of the alumina-supported metals as observed during disproportionation of dimethylamine (DMA) and monomethylamine (MMA), respectively. For both reactants, all three catalysts exhibit a drastic deactivation if the hydrogen in the feed is substituted by helium. Similar deactivation patterns were obtained when performing the same experiments with the pure metal powders. The deactivation of the copper catalyst appears to be reversible, whereas with cobalt and in particular with nickel the deactivation is only partly reversible with hydrogen. The small loss in activity of the copper catalyst after regeneration with hydrogen could be completely attributed to sintering of the copper particles as was evidenced by X-ray diffraction line broadening measurements, which indicated that the mean particle size increased from 15 to 19 nm. The deactivated alumina-supported nickel and cobalt catalysts exhibited a significant decrease of the BET-surface area as measured by nitrogen adsorption. With Ni/Al_2O_3, it decreased from 198 to 19 m^2/g, and, for Co/Al_2O_3, a decrease from 130 to 84 m^2/g was measured. The drastic decrease of the surface area measured for Ni/Al_2O_3 is ascribed to the occurrence of extensive pore mouth plugging, as was indicated by comparative pore-size distributions obtained by capillary condensation measurements carried out on fresh and deactivated catalyst using nitrogen.

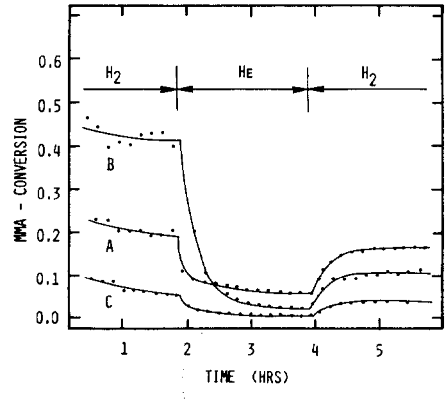

FIG. 2. Deactivation of alumina-supported metal catalysts during disproportionation of monomethylamine. For conditions, see Fig. 1.

It is interesting to note that the activity patterns of the catalysts were not the same for disproportionation of dimethylamine and monomethylamine. The copper catalyst was particularly active for the disproportionation of dimethylamine, whereas nickel showed the highest activity for the disproportionation and hydrocracking of monomethylamine.

B. Interaction of Methylamines with Metal Catalysts

In order to understand the origin of the catalyst deactivation, the interaction of dimethylamine with unsupported and alumina-supported metal catalysts was investigated by means of temperature-programmed desorption (TPD) and temperature-programmed surface reaction (TPSR).

Alumina support. In a first step the desorption from the pure alumina support was investigated after it was exposed to dimethylamine at 510 K under the same conditions as used for the deactivation experiments. Only desorption of dimethyla-

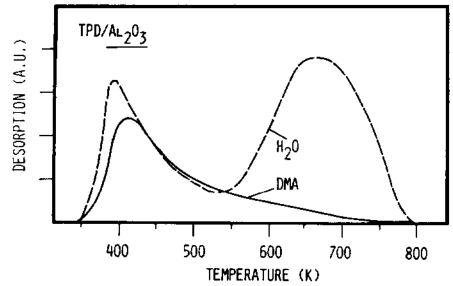

FIG. 3. Desorption of dimethylamine (DMA) and water from alumina support after deactivation experiment at 510 K.

mine and water was observed during these TPD measurements, as shown in Fig. 3. The water desorption curve exhibited the same shape as the one obtained with alumina which had not been exposed to dimethylamine. Only one significant dimethylamine desorption maximum is observed at about 415 K.

Copper catalyst. Figure 4 depicts the desorption curves measured for deactivated copper powder. In contrast to the desorption from the alumina, nitrogen desorption is observed in addition to the desorption of dimethylamine. About the same temperature for maximum nitrogen desorption is found as in earlier studies (*7*) where the desorption after exposure to ammonia was investigated. In that work it was shown by differential scanning calorimetry that the surface copper nitride starts to decompose exothermally at about 580 K in nitrogen (100 kPa). In a recent study (*12*) on the formation and decomposition of bulk copper nitride we found that in a nitrogen atmosphere (100 kPa) and at a heating rate of 0.084 K/s bulk copper nitride started to decompose at about the same temperature. In a hydrogen atmosphere (100 kPa), however, the commencement of the reduction of the bulk nitride could already be observed at about 390 K.

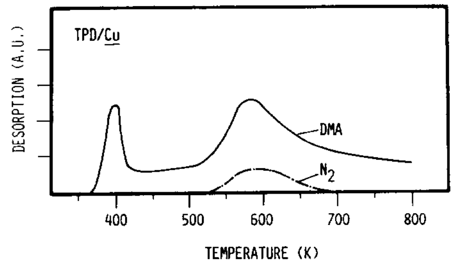

FIG. 4. Desorption of dimethylamine (DMA) and nitrogen from deactivated copper powder.

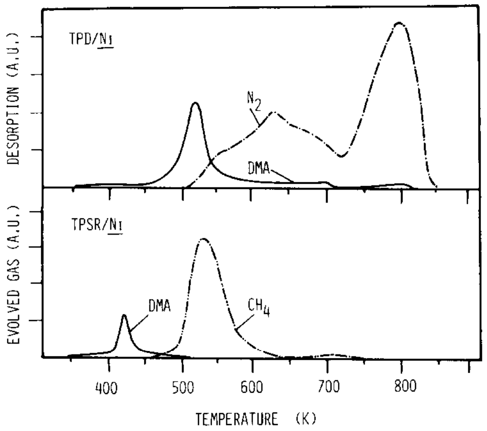

FIG. 5. Desorption of dimethylamine (DMA) and nitrogen, and evolution of methane from deactivated nickel powder observed with TPD and TPSR.

The desorption of dimethylamine from the deactivated copper powder (Fig. 4) shows two maxima, the first appearing at about 390 K and the second at about 580 K. The latter desorption peak does not appear with dimethylamine desorption from the alumina support (see Fig. 3).

Nickel catalysts. The TPD and TPSR profiles measured with deactivated nickel powder are presented in Fig. 5. With TPD, desorption of dimethylamine and nitrogen is observed. In contrast to the desorption from deactivated copper, only one desorption maximum is observed for dimethylamine, but two for nitrogen desorption. Nitrogen desorbs in the temperature range 600–800 K where the decomposition of nickel nitride formed by interaction of nickel with ammonia has been observed by means of differential scanning calorimetry (*7*). The TPSR measurement shows, in particular, methane formation with a maximum rate at about 540 K and dimethylamine desorption at considerably lower

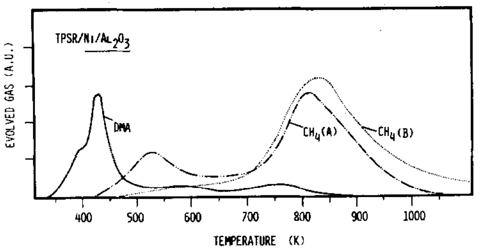

FIG. 6. Evolution of dimethylamine (DMA) and methane form deactivated Ni/Al_2O_3. Effect of heat treatment (770 K for 2 h) before the TPSR measurement.

temperature than observed in the TPD measurements. The presence of hydrogen enhances the desorption of dimethylamine, probably due to recombination of a π-bonded surface intermediate $H_2C \mathrel{+\!\!\!\!=} NCH_3$ with hydrogen. The latter surface intermediate has already been suggested to be active in the disproportionation reaction in the excellent study by Anderson and Clark (*13*) on reactions of aliphatic amines over evaporated metal films. In addition to methane formation and desorption of dimethylamine small amounts of disproportionation products such as ammonia and monomethylamine were also detected at about the same temperature where methane evolution was observed. For the sake of clarity these curves were not plotted in Fig. 5.

X-Ray powder diffraction measurements carried out with the deactivated nickel powder exhibited only nickel carbide (Ni_3C) reflections indicating that the bulk nickel has been largely transformed to nickel carbide. Thus we believe that the methane evolution observed with maximum rate at 540 K is mainly due to reduction of the nickel carbide.

Figure 6 depicts the TPSR profiles measured for the Ni/Al_2O_3 catalyst after deactivation during disproportionation of dimethylamine. The dimethylamine evolution curve is only slightly different from the one obtained with the deactivated nickel powder shown in Fig. 5. Two different methane evolution curves are shown; curve A was obtained directly with the deactivated Ni/Al_2O_3, while curve B was measured after the deactivated Ni/Al_2O_3 was annealed for 2 h at 770 K in nitrogen (100 kPa). Curve A exhibits two significant maxima in the methane evolution, the first appearing at about 540 K, the second at about 820 K. This indicates that at least two different carbon species have to be distinguished with respect to their reactivity toward hydrogen. The ratio of the methane evolution originating from the hydrogenation of these two carbon species indicates that the less reactive form was populating the Ni surface about twice as much (ratio 2 : 1) as the more reactive form. The existence of these two distinguishable carbon forms explains the regeneration behaviour observed for the Ni/Al_2O_3 catalyst.

A comparison of the methane evolution curves (A) and (B) shown in Fig. 6 indicates that annealing the deactivated Ni/Al_2O_3 before taking the TPSR measurement caused conversion of the more reactive carbon species into the less reactive form. The methane evolution observed at lower temperature (540 K, curve A) disappeared completely with heating and was accompanied by an increase of the methane evolution taking place at higher temperature 820 K. With both TPSR measurements (curves A and B) the integral amount of methane formed was roughly the same, indicating that no substantial amount of the carbon converted to an unreducible form during the heat treatment.

A similar effect of the heat treatment on the reactivity of the carbon species toward hydrogen has already been observed by Rabo *et al.* (*14*). It is also consistent with the slow conversion of chemisorbed carbon atoms and carbidic carbon into amorphous carbon at temperatures above 600 K, as was reported by McCarty and Wise (*15*).

In contrast to the deactivated nickel powder, X-ray diffraction measurements of the deactivated Ni/Al_2O_3 did not show the reflections of Ni_3C, indicating that, at least, no bulk nickel carbide (Ni_3C) was present. The X-ray diffraction analysis revealed,

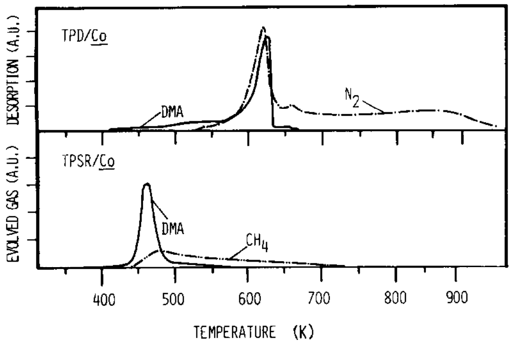

FIG. 7. Desorption of dimethylamine (DMA) and nitrogen, and evolution of methane from deactivated cobalt powder observed with TPD and TPSR.

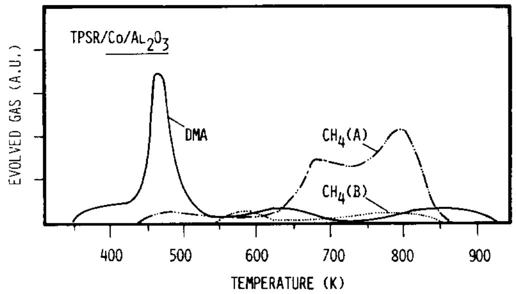

FIG. 8. Evolution of dimethylamine (DMA) and methane from deactivated Co/Al_2O_3. Effect of heat treatment (770 K for 2 h) before the TPSR measurement.

however, an expansion of the nickel lattice due to incorporation of carbon. The lattice constant of the nickel, a_0 = 3.52 Å, increased to 3.66 Å. With the heat treatment at 770 K this lattice expansion completely disappeared and nickel reflections (a_0 = 3.52 Å) were obtained in the X-ray diffraction analysis. Apparently, the heat treatment caused migration of the incorporated carbon to the nickel surface. Unfortunately, no decisive conclusion can be drawn from our investigation about the structure of the carbonaceous deposits hydrogenated at higher temperature. Considering its reactivity toward hydrogen, however, it seems likely that the bulk of the carbonaceous material consisted of amorphous carbon.

Cobalt catalysts. The TPD and TPSR results obtained with deactivated cobalt powder are summarized in Fig. 7. As with the nickel catalysts only a single significant desorption peak is observed for the dimethylamine, and at least two significant peaks can be distinguished for the desorption of nitrogen. The larger peak for nitrogen desorption appears at about 620 K. In contrast to the nickel powder, with the deactivated cobalt powder the methane formation during the TPSR experiment is relatively small and occurs between 450 and 730 K. As observed with the other metal catalysts, the desorption of dimethylamine is shifted to lower temperature in the presence of hydrogen.

The following results emerge from the TPSR measurements performed with the deactivated Co/Al_2O_3 catalyst shown in Fig. 8. The methane formation rate shows two significant maxima, the first appearing at 690 K and the second at 800 K. Heat treatment of the deactivated Co/Al_2O_3 sample before the TPSR measurement leads to an almost complete disappearance of methane formation indicating conversion of the reducible carbon species into an unreactive form. A similar curve for the desorption of the dimethylamine is measured as with the Ni/Al_2O_3 catalyst, showing an enhancement of the dimethylamine desorption in the presence of hydrogen.

The disappearance of the methane formation after heat treatment of the deactivated Co/Al_2O_3 may be explained by formation of a carbide which decomposes during the thermal treatment and forms carbonaceous deposits which cannot be reduced under the given conditions. The deactivated cobalt catalysts were not analysed by X-ray diffraction and therefore this explanation remains speculative. Carbide formation has, however, been detected by Renshaw *et al.* (*16*) on cobalt single crystal surfaces on which carbon was deposited by interaction with a CO/H_2 gas mixture.

C. Nature and Significance of Deactivation

Three deactivation processes have to be considered to explain the deactivation of

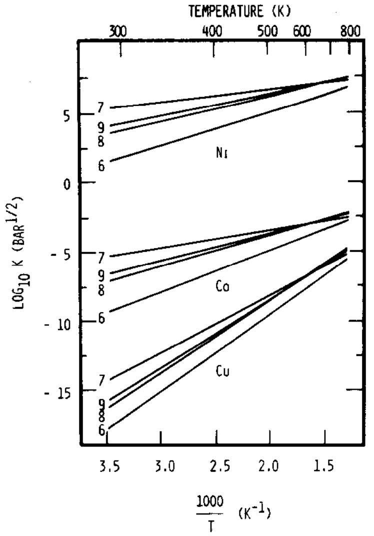

FIG. 9. Van't Hoff plots of reactions leading to metal nitrides. (Numbers indicate reactions (6)–(9) to the corresponding metal nitrides.)

the metal catalysts during disproportionation in the absence of hydrogen; these are, on the one hand, the formation of inactive metal nitrides and, on the other, the formation of carbonaceous deposits and metal carbides.

The metal nitrides may be formed either by reaction of the ammonia originating from the disproportionation or by direct reaction of the reactant amines such as methylamine or dimethylamine with the metal surface according to Eqs. (6)–(9).

$$NH_3 + 3\ Me \rightleftharpoons Me_3N + \tfrac{3}{2}\ H_2 \quad (6)$$

$$3\ (CH_3)_2NH + 3\ Me \rightleftharpoons 2\ N(CH_3)_3 + Me_3N + \tfrac{3}{2}\ H_2 \quad (7)$$

$$2\ CH_3NH_2 + 3\ Me \rightleftharpoons (CH_3)_2NH + Me_3N + \tfrac{3}{2}\ H_2 \quad (8)$$

$$\tfrac{3}{2}\ CH_3NH_2 + Me \rightleftharpoons \tfrac{1}{2}\ N(CH_3)_3 + Me_3N + \tfrac{3}{2}\ H_2 \quad (9)$$

A thermodynamic consideration of these reactions based on calculations from literature data (*17–21*) is presented in Fig. 9. The van't Hoff plots indicate that all reactions leading to metal nitrides are thermodynamically feasible under amination (*4*) or disproportionation conditions. Hence, it seems very likely that all these reactions can contribute to the nitride formation observed with all three metal catalysts. The thermodynamic calculations shown in Fig. 9 reveal that only a small hydrogen partial pressure is necessary to prevent nitride formation.

In contrast to the nitride formation, the formation of carbonaceous deposits and/or metal carbides is obtained only with the nickel and cobalt catalysts. These processes lead to irreversible deactivation due to carbonaceous deposits which are not reducible under amination or disproportionation conditions.

ACKNOWLEDGMENT

Financial support by the Swiss National Science Foundation (Grant 2.806-0.80) is gratefully acknowledged.

REFERENCES

1. Kliger, G. A., Lazutina, L. F., Fridman, R. A. Kryukow, Y. B., Bashkirov, A. N., Snagovskii, Y. S., and Smirnova, R. M., *Kinet. Catal. (Engl. Transl.)* **16,** 567 (1975).

2. Baiker, A., and Richarz, W., *Ind. Eng. Chem. Prod. Res. Dev.* **16,** 261 (1977).

3. Ono, Y., and Ishida, H., *J. Catal.* **72,** 121 (1981).

4. Baiker, A., Caprez, W., and Holstein, W. L., *Ind. Eng. Chem. Prod. Res. Dev.* **22,** 217 (1983).

5. Pommersheim, J. M., and Coull, J., *AIChE J.* **17,** 1075 (1971).

6. Volf, J., Pasek, J., and Duraj, N., *Collect. Czech. Chem. Commun.* **38,** 1038 (1973).

7. Baiker, A., *Ind. Eng. Chem. Prod. Res. Dev.* **20,** 615 (1981).

8. Baiker, A., and Richarz, W., *Synth. Commun.* **8,** 27 (1978).

9. Baiker, A., and Monti, D., *Ber. Bunsenges. Phys. Chem.* **87,** 602 (1983).

10. Monti, D., and Baiker, A., *J. Catal.* **83,** 323 (1983).

11. Rau, R. C., *in* "Encyclopedia of X-Rays and γ-Rays" (G. L. Clark, Ed.), p. 184. Reinhold, New York, 1963.

12. Baiker, A., and Maciejewski, M., *J. Chem. Soc. Faraday Trans. I,* in press.

13. Anderson, J. R., and Clark, N. J., *J. Catal.* **5,** 250 (1966).

14. Rabo, J. A., Risch, A. P., and Poutsma, M. L., *J. Catal.* **53,** 295 (1978).

15. McCarty, J. G., and Wise, H., *J. Catal.* **57,** 406 (1979).

16. Renshaw, G. D., Roscoe, C., and Walker, P. L., *J. Catal.* **22**, 394 (1971).
17. Stull, D. R., Westrum, E. F., and Sinke, G. C., "The Chemical Thermodynamics of Organic Compounds." Wiley, New York, 1969.
18. Vorob'ev, A. M., Evseeva, G. V., and Zenkevich, L. V., *Zh. Fiz. Khim.* **47** (10), 2708 (1973).
19. Barin, I., Knacke, O., and Kubaschewski, O., "Thermochemical Properties of Inorganic Substances," Supplement, p. 182. Springer-Verlag, Berlin, 1977.
20. Hahn, H., and Konrad, A., *Z. Anorg. Allg. Chem.* **264**, 181 (1951).
21. Searcy, A. W. *in* "Chemical and Mechanical Behaviour of Inorganic Materials" (A. W. Searcy, D. V. Ragone, and U. Colombo, Eds.), p. 1. Wiley, New York, 1970.